

Combining density-based dynamical correlation with a reduced-density-matrix strong-correlation description

Robert van Meer ^{1,*}, Oleg Gritsenko,^{2,3} and Jeng-Da Chai ^{1,4,†}

¹Department of Physics, National Taiwan University, Taipei 10617, Taiwan

²Section Theoretical Chemistry, VU University, NL-1081 HV Amsterdam, The Netherlands

³Institute of Physics, Lodz University of Technology, PL-90-924 Lodz, Poland

⁴Center for Theoretical Physics and Center for Quantum Science and Engineering, National Taiwan University, Taipei 10617, Taiwan



(Received 8 July 2020; accepted 26 August 2020; published 15 September 2020)

A combined density and density-matrix functional method is proposed for the calculation of potential energy curves of molecular multibond dissociation. Its density-matrix part, a pair-density functional, efficiently approximates the *ab initio* pair density of the complete active space (CAS) method. The corresponding approximate on-top pair density Π is employed to correct for double counting in the correlation energy functional. The proposed ELS+ method, which augments the extended Löwdin-Shull (ELS) density-matrix functional with the Π -based scaled density functional, closely reproduces potential curves of the paradigmatic multibond dissociation in N_2 , H_2O , and H_2CO molecules calculated with the recently proposed CAS Π DFT [CAS augmented with the Π -based scaled correlation correction of density functional theory (DFT)] method. Furthermore, with the additional correction for the intrafragment correlation between the broken-bond electrons, ELS + + reproduces well the benchmark potential curve of the N_2 molecule by Lie and Clementi.

DOI: [10.1103/PhysRevA.102.032815](https://doi.org/10.1103/PhysRevA.102.032815)

I. INTRODUCTION

The adequate description of bond-breaking processes often requires the correct handling of both dynamical and strong nondynamical correlation at all bond distances. Conventional Kohn-Sham density functional theory (DFT) [1,2] employing approximate density functionals is fully capable of handling the (mainly) dynamical correlation for equilibrium geometry structures but fails to deliver an adequate description of the strong correlation that is required when one dissociates bonds [3,4]. Recently, thermally assisted occupation DFT (TAO-DFT) [5–7], an efficient method to describe both dynamical and strong nondynamical correlation [8,9], has been developed. However, the choice of the fictitious temperature which among other things determines the orbital occupation numbers through Fermi-Dirac statistics in TAO-DFT remains difficult, especially for molecular multibond dissociation [10].

Alternatively, an effective way of describing the strong correlation using a functional-like description is to use density matrix functional theory (DMFT) [11–23], not to be confused with dynamical mean field theory. In DMFT, the electronic energy is expressed as a functional of the one-body reduced density matrix components, allowing for more flexibility than just using the density. The most successful earlier JK-only functionals [17,24] using in their energy expressions only two-electron integrals with the Coulomb and exchange-type orbital products (see Sec. II) were capable of generating most of the dynamical correlation for single bonds. However, this

type of functional does not provide a reliable description of dissociation of multiple bonds. Recent geminal-based approximate DMFT functionals are capable of describing multiple bond breaking but fail to describe 50–80% of the dynamical correlation and there does not seem to be a way to tackle dynamical correlation problem in a fully self-consistent fashion [22,25]. In this paper, we look at the previously developed CAS Π DFT method (*vide infra*) for guidance [26–28], and try to combine both functional approaches in order to obtain a functional based method that combines the best of both worlds and can generate rather accurate potential energy surfaces.

In the CAS Π DFT method, the electronic energy of a state is expressed in terms of the CAS self-consistent-field (CASSCF) energy E_e^{CASSCF} and the Π DFT component E^{PDFT} . The latter accounts for the dynamical correlation part which is not described by the CASSCF wave function

$$E_e^{\text{CAS}\Pi\text{DFT}} = E_e^{\text{CASSCF}} + E^{\text{PDFT}}[X^{\text{CASSCF}}, \rho^{\text{CASSCF}}]. \quad (1)$$

The Π DFT component itself is generated by using the scaled correlation energy density functional by Lee, Yang, and Parr (LYP) [29]

$$E^{\text{PDFT}}[X, \rho] = \int P[x] \epsilon_c^{\text{LYP}}[\rho(\mathbf{r})] d\mathbf{r}, \quad (2)$$

whose scaling factor $P[X]$ depends on the on-top density (pair-density $\Pi(\mathbf{r}_1, \mathbf{r}_2)$ evaluated at $\mathbf{r}_1 = \mathbf{r}_2$ [26,30–33]) and density ρ

$$X(\mathbf{r}) = \frac{2\Pi(\mathbf{r}, \mathbf{r})}{\rho(\mathbf{r})^2}. \quad (3)$$

*Corresponding author: rvanmeer@gmail.com

†Corresponding author: jdchai@phys.ntu.edu.tw

The currently used parametrization differentiates between two regions based on physical characteristics

$$P[X] = \begin{cases} P^{\text{SDC}}(X) \leq 1, X \leq 1 \\ P^{\text{EDC}}(X) > 1, X > 1 \end{cases}. \quad (4)$$

In case ($X \leq 1$), one is dealing with suppressed dynamical correlation (SDC), which is a situation that commonly occurs when bonds are being broken. The other scenario ($X > 1$) mainly occurs in energetically important spatial regions when one is describing distributed ionic type states, such as the first $^1\Sigma_u^+$ state of the H_2 molecule. In this case, an enhanced dynamical correlation (EDC) description is warranted.

The CASPDFT method with its suppression and enhancement of dynamical correlation has been applied successfully to various ground and excited state systems. The latest variants, CASPDFT + M and CAS(M)PDFT, which also include an additional medium distance correlation correction, have been able to fairly accurately reproduce complete basis set (CBS) limit potential energy curves for multibonded molecules [34,35].

Up until this point, the PDFT scheme has always been used in conjunction with a wave-function-based CAS-type (SCF or non-SCF) nondynamical correlation carrier. These carriers are relatively complicated, in the sense that they do not scale well with respect to an increase of the active space size, and they tend to generate a large number of pair density components that are more or less equivalent and thus should be lumped together [22]. In the case of ground states, one can also consider using a less complicated functional-based approach whose approximate energy, pair-density and concomitant on-top density and density quantities closely resemble the CASSCF quantities. The most suitable candidate is DMFT.

In this paper, we combine the DMFT approach with the PDFT dynamical correlation correction. Section II describes the methodical details of the density matrix functional that is used for all calculations, extended Löwdin-Shull (ELS) with dispersion and multibond corrections (DM), and its utilization of the PDFT correction scheme. In Sec. III, the full computational details of this endeavor are given. Section IV describes the application of the combined ELS+ scheme to several prototypical H_2O , N_2 , and H_2CO molecules and compares the results with the CASSCF + PDFT and CBS benchmark data. Conclusions are drawn in the final section.

II. DENSITY MATRIX FUNCTIONAL THEORY AND THE PDFT CORRECTION

In DMFT, the electronic ground-state energy can be written as a functional of the one-body reduced density matrix $\gamma(\mathbf{x}, \mathbf{x}')$ [36],

$$E_e^{\text{DMFT}}[\gamma(\mathbf{x}, \mathbf{x}')] = -\frac{1}{2} \int \nabla_{\mathbf{r}'}^2 \gamma(\mathbf{x}, \mathbf{x}')|_{\mathbf{x}'=\mathbf{x}} d\mathbf{x} + \int v_{\text{ext}} \gamma(\mathbf{x}, \mathbf{x}')|_{\mathbf{x}'=\mathbf{x}} d\mathbf{x} + W^{\text{DMFT}}[\gamma(\mathbf{x}, \mathbf{x}')]. \quad (5)$$

Here \mathbf{x} stands for the combination of the spatial \mathbf{r} and spin s electron coordinates, and $W_{\text{DMFT}}[\gamma(\mathbf{x}, \mathbf{x}')]]$ is the two-electron

interaction functional, whose exact form is only known for systems consisting of two electrons, requiring one to use approximate functionals for other systems. Several approximate functionals have been developed over the course of many years [12–23]. All of these functionals can essentially be written as an integral over the approximate pair density in the natural orbital (NO) basis whose elements are determined by one-body density matrix quantities:

$$W^{\text{DMFT}}[\gamma(\mathbf{x}, \mathbf{x}')] = \int d\mathbf{r}_1 d\mathbf{r}_2 \frac{\Pi^{\text{DMFT}}[\gamma(\mathbf{x}, \mathbf{x}')](\mathbf{r}_1, \mathbf{r}_2)}{|\mathbf{r}_1 - \mathbf{r}_2|}. \quad (6)$$

The best candidate functional for our case is the ELS-DM functional, since it has been shown that this functional is fully capable of reproducing small CASSCF wave-function results for small molecules [22]. This functional is essentially an antisymmetrized product of strongly orthogonal geminals (APSG) functional with additional dispersive dynamical correlation (D) and multibond dissociation (M) corrections:

$$\Pi^{\text{ELS-DM}}(\mathbf{r}_1, \mathbf{r}_2) = \Pi^{\text{APSG}}(\mathbf{r}_1, \mathbf{r}_2) + \Pi^{\text{D}}(\mathbf{r}_1, \mathbf{r}_2) + \Pi^{\text{M}}(\mathbf{r}_1, \mathbf{r}_2). \quad (7)$$

The APSG functional [37,38] divides the system into multiple two-electron subsystems with their own set of natural orbitals (NOs), the density-matrix eigenfunctions. It uses the exact two-electron Löwdin-Shull (LS) functional for the interaction of the orbitals (and electrons) within the set [39], and a Hartree-Fock (HF) type of interaction (no correlation) between orbitals belonging to different sets

$$\Pi^{\text{APSG}}(\mathbf{r}_1, \mathbf{r}_2) = \sum_{P < Q} \sum_{i \in P} \sum_{j \in Q \neq P} n_i n_j (4j_{ij}(\mathbf{r}_1, \mathbf{r}_2) - 2k_{ij}(\mathbf{r}_1, \mathbf{r}_2)) + \sum_P \sum_{i \in P} \sum_{j \in P} f_i f_j \sqrt{n_i n_j} l_{ij}(\mathbf{r}_1, \mathbf{r}_2). \quad (8)$$

Here P and Q denote geminal NO sets, f_i are the phase factors that have a value of 1 for the first member of a set and generally -1 for all other members of the set, $\phi_i(\mathbf{r})$ are the NOs, and n_i are the natural occupation numbers (NONs) whose value ranges from 0 to 1. The Coulomb j_{ij} , exchange k_{ij} , and star swapped exchange l_{ij} orbital products lead to their respective integrals when integrated, and are given by

$$j_{ij}(\mathbf{r}_1, \mathbf{r}_2) = \phi_i^*(\mathbf{r}_1) \phi_j^*(\mathbf{r}_2) \phi_i(\mathbf{r}_1) \phi_j(\mathbf{r}_2), \quad (9)$$

$$k_{ij}(\mathbf{r}_1, \mathbf{r}_2) = \phi_i^*(\mathbf{r}_1) \phi_j^*(\mathbf{r}_2) \phi_j(\mathbf{r}_1) \phi_i(\mathbf{r}_2), \quad (10)$$

$$l_{ij}(\mathbf{r}_1, \mathbf{r}_2) = \phi_i^*(\mathbf{r}_1) \phi_j(\mathbf{r}_2) \phi_j(\mathbf{r}_1) \phi_i^*(\mathbf{r}_2). \quad (11)$$

Note that the difference between the k_{ij} and l_{ij} orbital products only plays a role for the time-dependent treatment [40–43] and is not important for the rest of this paper. The occupation numbers of the APSG functional follow a strict sum rule,

$$\sum_{i \in P} n_i = 1, \quad (12)$$

ensuring that each geminal-set contains exactly two electrons (total occupation of 1 in our notation). While one can in principle assign any number of orbitals to a given geminal, one often resorts to only assigning two orbitals to every geminal (perfect pairing) due to the ambiguity of the assignment of

more orbitals and the often relatively little energetic gain when doing so.

The Π^M correction to the APSG functional represents the contribution to Π which is required to restore the (often) physically correct local high spin exchange interaction between bond broken electrons on the same dissociated fragment [22]

$$\begin{aligned} \Pi^M(\mathbf{r}_1, \mathbf{r}_2) = & - \sum_{P < Q} \sum_{i \in P} \sum_{j \in Q \neq P} k_{ij} P_m(n_i(1-n_i)) P_m \\ & \times (n_j(1-n_j)) \sqrt{n_i(1-n_i)n_j(1-n_j)}. \end{aligned} \quad (13)$$

Here

$$P_m(z) = \left(1 + \frac{16}{\gamma}\right) \frac{\gamma z^2}{1 + \gamma z^2} \quad (14)$$

and γ is a parameter. The Π^D correction describes the dynamical dispersion type of correlation between electrons on different geminals and is responsible for up to 50% of the CASSCF equilibrium geometry correlation in case one uses an active space of 1 orbital for each valence electron

$$\Pi^D(\mathbf{r}_1, \mathbf{r}_2) = \frac{1}{2} \sum_{P < Q} \sum_{i \neq a \in P} \sum_{j \neq b \in Q \neq P} F_D(n_i, n_a, n_j, n_b) d_{ia,jb}. \quad (15)$$

Here the dispersive type orbital product is given by

$$d_{ia,jb}(\mathbf{r}_1, \mathbf{r}_2) = \phi_i(\mathbf{r}_1) \phi_j(\mathbf{r}_2) \phi_a^*(\mathbf{r}_1) \phi_b^*(\mathbf{r}_2) \quad (16)$$

and the F_D prefactor is given by

$$F_D(n_i, n_a, n_j, n_b) = 8 f_{ia,jb} P_d(n_i n_a) P_d(n_j n_b) \sqrt{n_i n_a n_j n_b}, \quad (17)$$

where $f_{ia,jb}$ are phase factors that ensure that the energetic contribution of each index combination is negative (attractive). In (17), $P_d(z)$ are the following functions of the NON products,

$$P_d(z) = \alpha \left(1 - \frac{\beta z^2}{1 + \beta z^2}\right), \quad (18)$$

with α and β being the parameters (see below).

When both corrections are applied, one can reproduce the energies of small CASSCF expansions. One should keep in mind that these CASSCF expansions still only cover 50% of the dynamical correlation; the other half of this correlation can only be captured by somehow incorporating the correlation space of the remainder of the complete set of “virtual” orbitals. As already mentioned before, in the case of the APSG functional, this additional space can be quite hard (and pointless) to incorporate. One can often get only relatively little energetic gain, while the efficiency of the SCF process is slowed down significantly by the constant moving of orbitals between sets. The situation improves slightly when additional intergeminal correlation is introduced. However, the higher lying virtuals can still not be assigned to a specific set.

The most practical way to solve this issue is to use a method that does not require the set assignment of this “sea of virtuals.” There are essentially two main classes of these general dynamical correlation schemes that can be used: perturbative approaches and scaled DFT correlation energy functionals. Several perturbative approaches have been successfully applied to geminal-based functionals [21,44,45], the main downside being the relatively large dependence on the

size of the basis required for the proper account of dynamical correlation. Note that DFT-based approaches have a much smaller dependence on the basis set size, since they do not use unoccupied virtual orbitals. In our case, we use such a DFT-based approach and obtain the missing dynamical correlation by inserting the approximate ELS-DM on-top pair density of Eq. (7) and density into the Π DFT expression (2)

$$E_e^{\text{ELS}+} = E_e^{\text{ELS-DM}} + E^{\Pi\text{DFT}}[X^{\text{ELS-DM}}, \rho^{\text{ELS-DM}}] \quad (19)$$

with

$$X^{\text{ELS-DM}}(\mathbf{r}) = \frac{2\Pi^{\text{ELS-DM}}(\mathbf{r}, \mathbf{r})}{\rho^{\text{ELS-DM}}(\mathbf{r})^2}, \quad (20)$$

resulting in a method that is completely based on functional approaches and does not require large basis sets.

III. COMPUTATIONAL DETAILS

All CASSCF calculations have been performed using the GAMESS-US program [46]. The DMFT and Π DFT calculations have been performed by using a homemade program that accepts integrals and other quantities from GAMESS-US. The cc-pVTZ (no f function) basis has been used for all calculations, since this allows us to easily compare the results with a recently published Π DFT study [34]. This choice also allows us to use the parametrization that was used in this study. So $P^{\text{SDC}}(X)$, which governs the suppression of dynamical correlation, is given by

$$P^{\text{SDC}}(X) = \frac{ax}{1 + (a-1)x} \quad (21)$$

with $a = 0.2$, and $P^{\text{EDC}}(X)$, which governs the enhancement of dynamical correlation, is given by

$$P^{\text{EDC}}(X) = c \sqrt[4]{x} - \frac{(c-1)(x-g)^2}{(1-g)^2} \quad (22)$$

with $c = 2.6$ and $g = 1.5$.

The original parameters of the ELS-DM functional are given by [22]

$$\begin{aligned} \alpha_o &= 1.25, \\ \beta_o &= 750, \\ \gamma_o &= 1500. \end{aligned}$$

These parameters were optimized for reproducing CASSCF energies for CAS spaces of one orbital per valence electron. The Π DFT correction scheme has, in principle, only been applied to smaller active spaces of two orbitals per broken bond. In order to facilitate the comparison to earlier CAS Π DFT application, we restrict ourselves to the smaller active space. Simultaneously such a choice allows one to reparametrize the original parameters. The following modified parameters have been used to obtain better results in the intermediate bond distance regions for molecules with multiple broken bonds in the same region:

$$\begin{aligned} \alpha_m &= 1.1, \\ \beta_m &= 250, \\ \gamma_m &= 1500. \end{aligned}$$

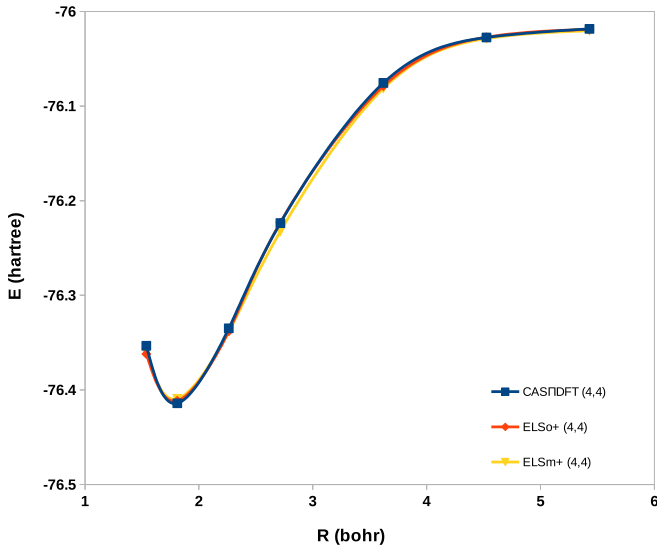


FIG. 1. H_2O double bond dissociation curves for an active space of four electrons in four orbitals. All curves depict total energies that include the Π DFT correction.

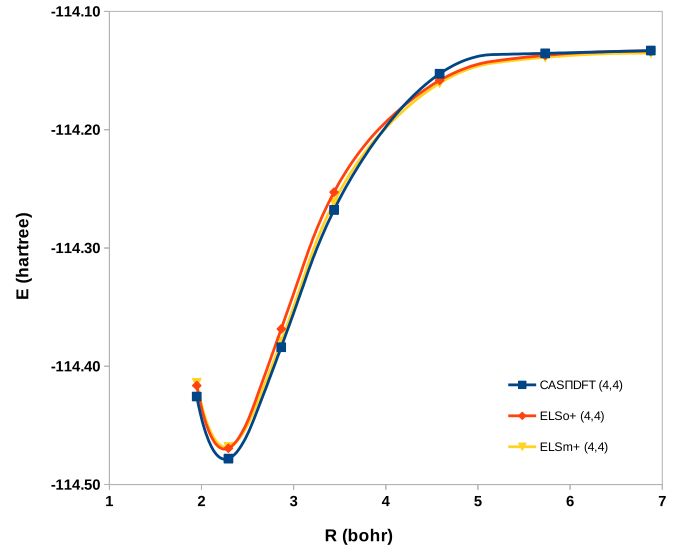


FIG. 2. H_2CO $\text{C}=\text{O}$ double bond dissociation curves for an active space of four electrons in four orbitals. All curves depict total energies that include the Π DFT correction.

In all cases, we show the results of both the original (o) and the modified (m) ELS-DM parametrization.

Geminal-based functionals do not use the same concept of active space as the CASSCF method, since one has to obey set restrictions. However, in the case of relatively isolated bonds or lone pairs, one can easily translate minimal CASSCF active spaces to the geminal set groupings. A single set is used for every two electrons in the system. If only a single orbital is assigned to a set, the geminal has no correlation at all and is essentially a frozen core orbital whose orbital shape can still be optimized. Throughout this paper, we have assigned a single orbital to a set for all orbitals that are not directly involved in the bond-breaking process. For orbitals that are involved in the bond-breaking process, we have assigned every bonding and corresponding antibonding orbital to a single set.

IV. RESULTS

In this section, we shall show the results of combining the ELS-DM DMFT functional with the Π DFT scheme for the H_2O (double bond break), N_2 , and H_2CO ($\text{C}=\text{O}$ bond break) molecules. All of these molecules contain multiple broken bonds. The reasons for choosing such a test set are that the exact DMFT functional for two electron systems is exactly equal to the CASSCF treatment and that the ELS-DM functional reduces to the exact functional if one only uses two active electrons, making the comparison between ELS-DM and CASSCF trivial if only single bond breaks with minimal active spaces were to be discussed.

It should be mentioned that the Π DFT scheme still has some caveats and it does not always recover all dynamical correlations. The focus of the DMFT-CASSCF comparison is quite reasonable since any corrections to the Π DFT scheme are more likely to be applicable to both the DMFT and CASSCF methods if all of the initial DMFT and CASSCF quantities are comparable. Below we will look at one of these corrections.

The total energy curves (CASSCF/DMFT + Π DFT) for a minimal active space of two orbitals per broken bond are shown in Figs. 1–3. The energy decomposition (CASSCF/DMFT, Π DFT, CASSCF/DMFT + Π DFT) of the N_2 , H_2O , and H_2CO molecules for three bond distances [equilibrium, roughly 1.5 times equilibrium (halfway dissociated) and roughly three times equilibrium (dissociated)] is shown in Table I.

We will begin our analysis with the H_2O molecule, for which two linked but isolated bonds are dissociated simultaneously. Both the original parameter (ELSo+) and modified parameter (ELSm+) ELS+ curves shown in Fig. 1 nearly coincide with the CAS Π DFT curve and Table I shows that

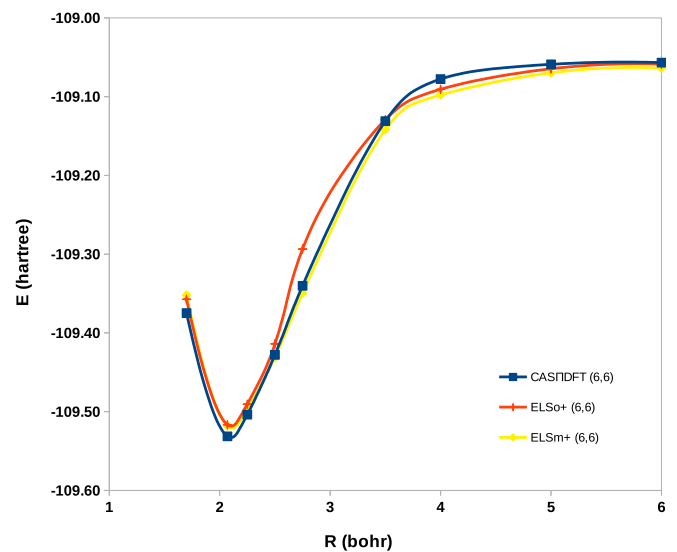


FIG. 3. N_2 triple bond dissociation curves for an active space of six electrons in six orbitals. All curves depict total energies that include the Π DFT correction.

TABLE I. Energies in hartree for minimal active space calculations. The CAS section shows the CASSCF energies and the DMFT energies that try to approximate it. The Π DFT section gives the dynamical correlation correction. The CAS + Π DFT section shows the sum.

| R (bohr) | | N_2 | | | H_2CO | | | H_2O | | |
|-----------------|---------|-----------|-----------|-----------|-----------|-----------|-----------|----------|----------|----------|
| | | 2.075 | 2.75 | 6.0 | 2.292 | 3.468 | 6.876 | 1.81 | 2.72 | 5.43 |
| CAS space | CASSCF | -109.1166 | -108.9732 | -108.7949 | -113.9816 | -113.8219 | -113.7331 | -76.1084 | -75.9549 | -75.8057 |
| | ELS-DMo | -109.1088 | -108.9455 | -108.7966 | -113.9749 | -113.8188 | -113.7336 | -76.1100 | -75.9564 | -75.8064 |
| | ELS-DMm | -109.1222 | -108.9909 | -108.8019 | -113.9781 | -113.8255 | -113.7354 | -76.1090 | -75.9664 | -75.8079 |
| Π DFT | CASSCF | -0.4148 | -0.3671 | -0.2620 | -0.4966 | -0.4460 | -0.4000 | -0.3058 | -0.2687 | -0.2127 |
| | ELS-DMo | -0.4078 | -0.3480 | -0.2621 | -0.4944 | -0.4340 | -0.4000 | -0.3014 | -0.2667 | -0.2125 |
| | ELS-DMm | -0.3958 | -0.3587 | -0.2620 | -0.4901 | -0.4359 | -0.3999 | -0.3005 | -0.2661 | -0.2124 |
| CAS + Π DFT | CASSCF | -109.5314 | -109.3402 | -109.0568 | -114.4782 | -114.2679 | -114.1331 | -76.4142 | -76.2236 | -76.0184 |
| | ELS-DMo | -109.5166 | -109.2935 | -109.0587 | -114.4693 | -114.2528 | -114.1336 | -76.4115 | -76.2230 | -76.0189 |
| | ELS-DMm | -109.5181 | -109.3496 | -109.0638 | -114.4682 | -114.2614 | -114.1353 | -76.4095 | -76.2325 | -76.0203 |

the individual components (CAS space and Π DFT correction) also nearly coincide, indicating that the combined ELS+ method can act as a substitute for CAS Π DFT for this molecule. One should note that the modified ELS-DM parametrization yields slightly inferior results compared to the original parametrization. This is not very alarming since the modified parametrization is mainly applicable to situations in which multiple bonds in the same region are broken.

The results for the C=O bond break of the H_2CO molecule paint a similar picture. The ELS+ energies and their decomposition are close to the CAS Π DFT ones. However, in this case the variation is slightly higher than for the H_2O case, especially at the equilibrium and intermediate bond distances.

The triple bond dissociation of the N_2 molecule proves to be a bit more difficult to describe for the ELS-DM functional. The original parametrization of the ELS-DM functional fails in the intermediate bond distance region. We analyzed the CASSCF 2RDM of this region and compared it to the original ELS-DM results and noted that the dispersive type interactions were present in CASSCF, while they were nearly absent for ELS-DM. The modified parameter set fixes this issue and yields good overall results.

We have seen that the ELS+ method is, after some reparametrization, capable of reproducing the CAS Π DFT results. However, as was mentioned before, the CAS Π DFT method is not without its errors. It has been shown that the dissociation limit of CAS Π DFT for multibonded systems is too high compared to the accurate CBS limit [34,35]. The main culprit is the lack of the interbond dynamical correlation between the electrons localized on the same fragment of a dissociating molecule. Two different correction schemes were proposed. The newest variant injects the density of the frontier orbitals into a LYP functional scaled by an occupation-number-dependent prefactor. The older variant, which we will be using here, essentially entails using the correlation correction for multibond systems, Eq. (13), again. The resulting CAS Π DFT + M method

$$E_e^{\text{CAS}\Pi\text{DFT}+M} = E_e^{\text{CAS}\Pi\text{DFT}} + \int d\mathbf{r}_1 d\mathbf{r}_2 \frac{\Pi^M[\gamma^{\text{CASSCF}}(\mathbf{r}, \mathbf{r}')](\mathbf{r}_1, \mathbf{r}_2)}{|\mathbf{r}_1 - \mathbf{r}_2|} \quad (23)$$

has shown to be capable of relatively accurately reproducing the CBS curve for the N_2 molecule. Similarly, one can add the correction (again) to the ELS+ method

$$E_e^{\text{ELS}++} = E_e^{\text{ELS}+} + \int d\mathbf{r}_1 d\mathbf{r}_2 \frac{\Pi^M[\gamma^{\text{ELS-DM}}(\mathbf{r}, \mathbf{r}')](\mathbf{r}_1, \mathbf{r}_2)}{|\mathbf{r}_1 - \mathbf{r}_2|}, \quad (24)$$

resulting in a method that ought to be able to reproduce the N_2 curve. As is shown in Fig. 4, this is indeed the case, proving that the ELS-DM functional is a satisfactory replacement for the CASSCF wave function for ground-state calculations.

V. CONCLUSIONS

A combined approximate density and density-matrix ELS++ functional method is proposed for calculation of potential energy curves of molecular multibond dissociation. It accounts for all relevant effects of electron correlation along

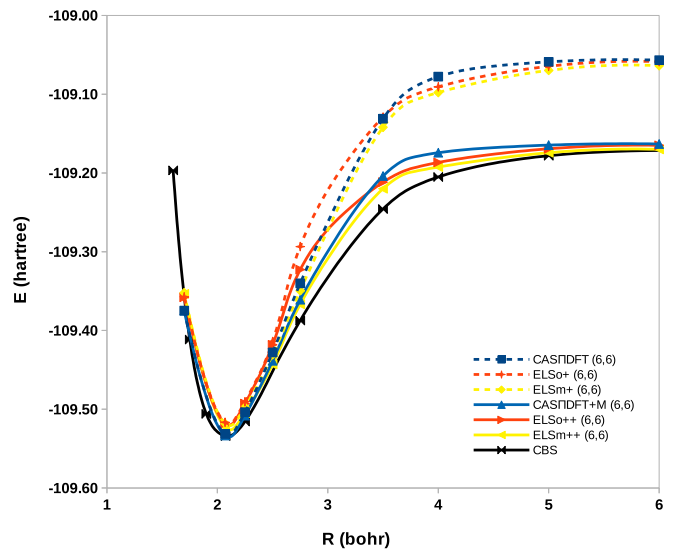


FIG. 4. N_2 triple bond dissociation curves for an active space of six electrons in six orbitals. All curves depict total energies that include the Π DFT correction. The dashed curves represent the calculations without the medium range correlation dissociation correction. The CBS data has been taken from Ref. [47].

the bond dissociation coordinate. These effects include the short-range dynamical correlation, the long-range intrabond nondynamical correlation, as well as the important in the dissociation region medium-range interbond electron correlation.

The key point of the present DMFT + DFT development is that the ELS-DM pair density, a relatively simple IRDM functional, closely reproduces a more complicated *ab initio* pair density of CASSCF. This allows the corresponding ELS-DM energy functional to efficiently account for nondynamical correlation.

Furthermore, the ELS-DM on-top pair density closely reproduces locally the CASSCF on-top pair density. This allows to physically meaningfully correct the correlation DFT LYP functional for SDC using the generated within DMFT on-top pair-density within PDFT.

The proposed ELS+(+) functionals are applied to the calculation of the potential energy curves of the multibond dissociation in the prototype molecules N_2 , H_2O , and H_2CO . The resultant potential energy curves go very close to the corresponding potential energy curves of the CASPDFT method, which has been recently successfully applied to the calculation of various molecular potential energy curves in Refs. [26,27,34,35].

The proposed ELS+(+) methods effectively resolve the major DMFT bottleneck, stemming from the troublesome feature of the IRDM spectrum, namely, the accumulation of the

NO eigenfunctions near the zero NON eigenvalue. Because of this feature, the two-step orbital and occupation number optimization scheme rarely converges fully. So reaching a fully self-consistent solution with a DM functional, which includes all NOs in a given basis, often becomes, in a general case, a veritable numerical nightmare.

The present ELS+(+) functionals efficiently circumvent this DMFT bottleneck by not using at all the higher NOs outside the minimal geminal subsets. In conventional DMFT, the inclusion of these NOs is required to properly account for dynamical correlation. At variance with this, in ELS+(+) dynamical correlation is evaluated with the PDFT functional, which does not use higher NOs. With the results obtained, this can be considered as a further development in the functional theory focused on the reliable calculation of the molecular potential energy curves.

ACKNOWLEDGMENTS

This work was supported by the Ministry of Science and Technology of Taiwan (Grant No. MOST107-2628-M-002-005-MY3), National Taiwan University (Grant No. NTU-CDP-105R7818), and the National Center for Theoretical Sciences of Taiwan. O.G. gratefully acknowledges the support by the Narodowe Centrum Nauki of Poland under Grant No. 2017/27/B/ST4/00756.

-
- [1] P. Hohenberg and W. Kohn, *Phys. Rev.* **136**, B864 (1964).
 [2] W. Kohn and L. J. Sham, *Phys. Rev.* **140**, A1133 (1965).
 [3] A. J. Cohen, P. Mori-Sánchez, and W. Yang, *Science (NY)* **321**, 792 (2008).
 [4] A. J. Cohen, P. Mori-Sánchez, and W. Yang, *Chem. Rev.* **112**, 289 (2012).
 [5] J.-D. Chai, *J. Chem. Phys.* **136**, 154104 (2012).
 [6] J.-D. Chai, *J. Chem. Phys.* **140**, 18A521 (2014).
 [7] J.-D. Chai, *J. Chem. Phys.* **146**, 044102 (2017).
 [8] C.-S. Wu and J.-D. Chai, *J. Chem. Theory Comput.* **11**, 2003 (2015).
 [9] C.-N. Yeh and J.-D. Chai, *Sci. Rep.* **6**, 30562 (2016).
 [10] C.-Y. Lin, K. Hui, J.-H. Chung, and J.-D. Chai, *RSC Adv.* **7**, 50496 (2017).
 [11] K. Pernal and K. J. H. Giesbertz, in *Density-Functional Methods for Excited States*, edited by N. Ferré, M. Filatov, and M. Huix-Rotllant (Springer International, Cham, 2016), pp. 125–183.
 [12] G. Csányi and T. A. Arias, *Phys. Rev. B* **61**, 7348 (2000).
 [13] A. M. K. Müller, *Phys. Lett. A* **105**, 446 (1984).
 [14] M. Buijse and E. J. Baerends, *Mol. Phys.* **100**, 401 (2002).
 [15] A. J. Cohen and E. J. Baerends, *Chem. Phys. Lett.* **364**, 409 (2002).
 [16] O. V. Gritsenko, K. Pernal, and E. J. Baerends, *J. Chem. Phys.* **122**, 204102 (2005).
 [17] D. R. Rohr, K. Pernal, O. V. Gritsenko, and E. J. Baerends, *J. Chem. Phys.* **129**, 164105 (2008).
 [18] N. N. Lathiotakis, S. Sharma, J. K. Dewhurst, F. G. Eich, M. A. L. Marques, and E. K. U. Gross, *Phys. Rev. A* **79**, 040501(R) (2009).
 [19] G. E. Scuseria and T. Tsuchimochi, *J. Chem. Phys.* **131**, 164119 (2009).
 [20] M. Piris, *J. Chem. Phys.* **141**, 044107 (2014).
 [21] M. Piris, *Phys. Rev. Lett.* **119**, 063002 (2017).
 [22] R. van Meer, O. V. Gritsenko, and E. J. Baerends, *J. Chem. Phys.* **148**, 104102 (2018).
 [23] R. van Meer and O. V. Gritsenko, *Phys. Rev. A* **100**, 032335 (2019).
 [24] M. Piris, J. M. Matxain, X. Lopez, and J. M. Ugalde, *J. Chem. Phys.* **133**, 111101 (2010).
 [25] V. A. Rassolov, F. Xu, and S. Garashchuk, *J. Chem. Phys.* **120**, 10385 (2004).
 [26] O. V. Gritsenko, R. van Meer, and K. Pernal, *Phys. Rev. A* **98**, 062510 (2018).
 [27] O. V. Gritsenko, R. van Meer, and K. Pernal, *Chem. Phys. Lett.* **716**, 227 (2019).
 [28] O. V. Gritsenko and K. Pernal, *J. Chem. Phys.* **151**, 024111 (2019).
 [29] C. Lee, W. Yang, and R. G. Parr, *Phys. Rev. B* **37**, 785 (1988).
 [30] P. Gori-Giorgi and A. Savin, *Phys. Rev. A* **73**, 032506 (2006).
 [31] R. K. Carlson, D. G. Truhlar, and L. Gagliardi, *J. Phys. Chem. A* **121**, 5540 (2017).
 [32] A. Ferté, E. Giner, and J. Toulouse, *J. Chem. Phys.* **150**, 084103 (2019).
 [33] D. R. Alcoba, A. Torre, L. Lain, O. B. Oña, E. Ríos, and G. E. Massaccesi, *Int. J. Quantum Chem.* **120**, e26256 (2020).
 [34] K. Pernal, O. V. Gritsenko, and R. van Meer, *J. Chem. Phys.* **151**, 164122 (2019).
 [35] M. Hapka, K. Pernal, and O. V. Gritsenko, *J. Chem. Phys.* **152**, 204118 (2020).

- [36] T. L. Gilbert, *Phys. Rev. B* **12**, 2111 (1975).
- [37] V. A. Rassolov, *J. Chem. Phys.* **117**, 5978 (2002).
- [38] K. Pernal, *Comput. Theor. Chem.* **1003**, 127 (2013).
- [39] P.-O. Löwdin and H. Shull, *Phys. Rev.* **101**, 1730 (1956).
- [40] K. Pernal, O. Gritsenko, and E. J. Baerends, *Phys. Rev. A* **75**, 012506 (2007).
- [41] K. Pernal and J. Cioslowski, *Phys. Chem. Chem. Phys.* **9**, 5956 (2007).
- [42] K. J. H. Giesbertz, O. Gritsenko, and E. J. Baerends, *J. Chem. Phys.* **136**, 094104 (2012).
- [43] R. van Meer, O. V. Gritsenko, and E. J. Baerends, *J. Chem. Phys.* **140**, 024101 (2014).
- [44] P. Jeszenszki, P. R. Nagy, T. Zoboki, A. Szabados, and P. R. Surjan, *Int. J. Quantum Chem.* **114**, 1048 (2014).
- [45] K. Chatterjee, E. Pastorzak, K. Jawulski, and K. Pernal, *J. Chem. Phys.* **144**, 244111 (2016).
- [46] M. W. Schmidt, K. K. Baldrige, J. A. Boatz, S. T. Elbert, M. S. Gordon, J. H. Jensen, S. Koseki, N. Matsunaga, K. A. Nguyen, S. Su, T. L. Windus, M. Dupuis, and J. A. Montgomery, *J. Comput. Chem.* **14**, 1347 (1993).
- [47] G. C. Lie and E. Clementi, *J. Chem. Phys.* **60**, 1288 (1974).